



Original Research

Enhanced photodynamic therapy by encapsulation of perfluorocarbon into PEGylated near-infrared dyes

Ke Jiang^{1,2#}, Haoran Wang^{1,2#}, Huanhuan Zhang^{1,2}, Yiqiao Hu^{1,2,3,4*}, Jinhui Wu^{1,2,3,4*}

¹ State Key Laboratory of Pharmaceutical Biotechnology, Medical School of Nanjing University, Nanjing University, Nanjing 210093, China

² Institute of Drug R&D, Medical School of Nanjing University, Nanjing 210093, China

³ Jiangsu Key Laboratory for Nano Technology, Nanjing University, Nanjing 210093, China

⁴ Jiangsu R&D platform for controlled & targeted drug delivery, Nanjing University, Nanjing 210093, China

Correspondence to: huyiqiao@nju.edu.cn, wuj@nju.edu.cn

Received March 20, 2018; Accepted July 17, 2018; Published July 30, 2018

These authors contributed equally to this work

Doi: <http://dx.doi.org/10.14715/cmb/2018.64.10.11>

Copyright: © 2018 by the C.M.B. Association. All rights reserved.

Abstract: Near-Infrared (NIR) dyes, with improved tissue penetration, minimal invasiveness and high specificity, have gained great interests in diagnosing and treating tumors. However, the poor solubility in aqueous medium and low ¹O₂ quantum yields of NIR dyes restrict their application in PDT (photodynamic therapy) research. Herein, a novel nanosystem with modifying the NIR dyes and encapsulating perfluorocarbon is reported for improving the PDT effectiveness of NIR dyes. By adding the PEG₂₀₀₀-SH and the C13 carbon chain to a NIR representative dye IR780, the new formed material PEG-IR780-C13 shows good solubility in water. Then PFTBA was encapsulated into PEG-IR780-C13 to form a nanosystem (PFTBA@PEG-IR780-C13). When exposed to laser irradiation, the nanosystem showed enhanced production of ¹O₂ and significantly increased PDT both in vivo and in vitro. Therefore, this work provides an approach for design and application of NIR dyes.

Key words: Encapsulated perfluorocarbon; PEGylated near-infrared dyes; Enhanced phototherapy; Anti-tumor therapy.

Introduction

Photodynamic therapy (PDT), an emerging photochemistry-involved treatment process for tumor and other diseases (1-3). In PDT, the photosensitizers (PS) is activated by light irradiation and it can transfer the absorbed energy to the surrounding molecular oxygen to generate singlet oxygen (¹O₂), which is a key cytotoxic agent to cells and tissues (4). Compared with photothermal therapy (PTT) and chemotherapy, PDT causes minimal invasiveness and toxicity to normal tissues because the generation of ¹O₂ is a light-triggered process and PS agents usually are not toxic in dark circumstances. The ideal PS should have good biocompatibility, high ¹O₂ quantum yield and long wavelength absorption for deep tumor penetration (5-7). However, the conventional PS used in PDT mostly activated by visible light or ultraviolet light, which has limited penetration depth in human tissues (1, 8-10). Consequently, these PS can only eradicate superficial tumors and hardly make the satisfactory progress in treating large and deep-seated tumors (11).

Near-Infrared (NIR) dyes, work in the region of spectrum between 700-1000nm (often called "optical window") (1,12). The advantages of using NIR dyes include minimal absorption by skins, tissues and cells, reduced scattering and enhanced penetration depth. The penetration depth of NIR dyes can reach to centimeter level. However, most NIR dyes have poor solubility in water and easily form aggregates in aqueous medium

(13). They generally have large π -conjugation domains that help them to self-assemble by π - π interaction resulting reduced ¹O₂ generation (14-15). The ¹O₂ quantum yield (Φ_{SO}) of NIR dyes is often less than 0.1. For instance, porphyrins, a liposome-mimicking nanoparticle self-assembled from porphyrin-phospholipid conjugates which exhibits high absorption of near-infrared light and diverse biophotonic applications (16-17) almost has no photodynamic effect, because the absorbed energy normally released via fluorescence and ¹O₂ was dissipated thermally (18).

To overcome these, we design a nanosystem by modifying the NIR dyes with PEG and long carbon chain (PEG-IR780-C13) to improve its solubility (19-20). PEGylation and long carbon chains can provide a higher solubility and better self-assemble capability of NIR dyes, significantly improve its stability in physiological environment (21-22). To improve its PDT effect, perfluorocarbon (PFC) was encapsulated (23, 26). PFC has good affinity to carbon chains, which helps it to be encapsulated easily into PEG-IR780-C13. Furthermore, PFC has a high oxygen solubility and has been used as an artificial blood substitute, which can provide enough oxygen for PS during PDT (23-25). More importantly, the ¹O₂ lifetime in PFC has been showed to be much longer than that in cellular environment or water (27). Therefore, the encapsulation of PFC in PEG-IR780-C13 can improve the PDT effects significantly. In this study, we investigated the photodynamic effect of PFTBA@PEG-IR780-C13 by evaluating ¹O₂ generation ability in

vitro and in vivo. We showed that this new approach may provide a clue to achieve an encouraging PDT therapeutic outcomes of typically NIR dyes.

Materials and Methods

Materials

PEG2000-SH purchased from Yarebio Ltd. (Shanghai, China). IR780-C13 synthesized by Heowns Business License (Tianjin, China). TEA (Triethylamine), IR780 were obtained from Sigma-Aldrich Co. LLC (USA). PFTBA (Perfluorotributylamine) was purchased from Meryer Chemical Technology Co Ltd (Shanghai, China), Singlet oxygen sensor green and 20, 70-dichlorodihydrofluorescein diacetate (H₂DCFDA) were both purchased from Invitrogen Corp. The BALB/c mice were purchased from Yangzhou University Medical Center (Jiangsu, China), and the weight of each mouse was 20–22g. CCK-8 (cell counting kit-8) was supplied by Dojindo Laboratories (Japan). TUNEL kit (TdT-mediated dUTP nick end labeling) was obtained from Roche Group.

Synthesis of PFTBA@PEG-IR780-C13

PEG-IR780-C13 was synthesized following our previous reported protocol. Briefly, IR-780-C13 (25mg), PEG2000-SH (60mg) and TEA (10ul) were mixed in 30ml chloroform, stirred for 24h, after removing the organic solvent and purified by column chromatography. The end-product was lyophilized to get the green powder. Then dissolve the obtained powder in deionized water to get the PEG-IR780-C13 aqueous solution. A certain number of PFTBA added into the solution and emulsified by ultrasonic cell crusher (XO-650D, Nanjing Atpio Instruments Manufacturer Corporation, China) at an ice bath for 6 mins (15). The concentration of PEG-IR780-C13 was quantified by UV–vis spectrophotometer (UV2450, Shimadzu Corporation, Japan).

Characterizations of PFTBA@PEG-IR780-C13

The morphology of PFTBA@PEG-IR780-C13 was characterized by transmission electron microscopy (Hitachi H-7650, Japan). The samples were dried on a copper grid coated with amorphous carbon and observed at 80 kV. The size distribution of PFTBA@PEG-IR-C13 was measured by Zetasizer Nano S90 (Malvern Instruments Ltd, UK). Gas chromatography–mass spectrometry (GC-MS) analysis was performed using a Clarus 680 gas chromatograph–mass spectrometer (PerkinElmer, Germany) equipped with an AxION® iQT™ detector. The fluorescence spectra of PEG-IR780-C13 and PFTBA@PEG-IR780-C13 were evaluated by using multifunctional microplate reader (Safire, TECAN) and IVIS Lumina imaging system (Xenogen Co., USA).

Single oxygen generation and detection in vitro

The commercial single oxygen (¹O₂) specific dye, singlet oxygen sensor green (SOSG, Invitrogen Corp, USA) was used to detect the ¹O₂ production. 20ul SOSG(50uM) and 100ul samples were mixed in 96-well plates and qualified by multifunctional microplate reader (Ex/Em=504/525 nm) after NIR (808nm, 2w/cm²) irradiation.

The photostability of PFTBA@PEG-IR780-C13

The absorption spectra of PEG-IR780-C13, PEG-IR780-C13 and IR780 solutions were determined by the UV–vis spectrophotometer after the 1 minute irradiation process or 2 days storage (in darkness)

ROS generation and detection in cancer cells

We pre-seeded Renca cells in a 12-well plate and incubated it for 24h at an atmosphere of 37 °C, 5% CO₂. Then incubated with PBS, PEG-IR780-C13 or PFTBA@PEG-IR780-C13 and Carboxy-H₂DCFDA (a widely used fluorogenic marker for reactive ROS), Hoechst 33342(a widely used fluorogenic marker for nucleus) for 30min, the concentration of PEG-IR780-C13 is 50ug/ml. Subsequently, we washed cells with PBS 2 times and exposed the corresponding groups to NIR irradiation for 40s. Fluorescence images of cells were captured by confocal fluorescence microscope (OLYMPUS FV1000). The fluorescence emission spectrum is carboxy-DCF (Ex/Em=495/529 nm) and Hoechst 33342 (Ex/Em=350/461 nm).

Flow cytometry

The Renca cells were pre-seeded in 12-well plates. After incubation for 24 h, PBS, PEG-IR780-C13, or PFTBA@PEG-IR780-C13 (concentration of PEG-IR780-C13=50ug/ml; PFTBA=1%, V/V) was added to corresponding well. Then the cells were incubated for 30 min at 37°C. After once washing with PBS, We added carboxy-H₂DCFDA (25 mM) to the cells and incubated it for 10 min. Subsequently, the cells were washed once with PBS and irradiated by NIR laser for 40s per well. The cells were then centrifuged, resuspended in 1 ml PBS and analyzed by flow cytometry (FACS-Calibur, BD Corp.). Data were obtained and analyzed using the CELLQUEST and FLOWJO programs.

Cytotoxicity experiments of PFTBA@PEG-IR780-C13 NPs in vitro

For the co-staining of live and dead cells, cells pre-seeded at a density of 1×10⁴ cells in 96-well plate and incubated with PBS, PEG-IR780-C13(50ug/ml) and PFTBA@PEG-IR780-C13(50ug/ml, 1% V/V PFTBA). After NIR irradiation, cells were stained with propidium iodide (PI, 20 μg/ml, stains dead cells only) and Calcein AM (5 μM/ml, stains live cells only) for 15 min at 37 °C. Then we washed the cells with PBS 2 times and observed it by the confocal fluorescence microscope (OLYMPUS FV1000).

To verify the cytotoxicity, Renca cells were maintained in RPMI 1640 medium supplemented with 10% (v/v) foetal bovine serum in a humidified 5% CO₂ atmosphere at 37 °C. These cells were seeded into a 96-well plate at a density of 5×10³ cells per well. After incubation for 24h, the cells were treated with PEG-IR780-C13 or PFTBA@PEG-IR780-C13 at different concentrations (20μl samples mixed with 100μl culture medium). Then the cells were immediately irradiated with 808-nm laser (2W/cm²) for 40s (4 cycles of 10s irradiation per well, 1 minute interval time was added between every twice irradiation). After co-incubation for 1h, drugs were removed and fresh culture medium was added. After 24 h incubation, the cell viability was performed by CCK-8. Cells treated by PBS without ir-

radiation was set as control.

Animals model

Male Balb/c mice were used under protocols approved by Nanjing University Laboratory Animal Center. Briefly, 1×10^7 CT26 cells in 0.2 ml PBS were subcutaneously injected into flank of mice. 14 days later, the tumor was isolated and cut into small blocks (about 1 mm^3) and implanted into the right flank of each mouse. When the size of tumor was around 70 mm^3 , the tumor bearing mice were used for the subsequent experiment. All relative experiments were carried out in accordance with the guidelines issued by the Institutional Animal Care and Use Committee (IACUC) of Nanjing University.

In vivo PDT therapy

Mice bearing CT26 tumors were randomly divided into six groups ($n=6$ each group). 40ul Saline, PEG-IR780-C13 (100ug/ml) and PFTBA@PEG-IR780-C13 (100ug/ml, PFTBA 5% v/v) was directly injected into the corresponding group's mice tumor mass. After injection, the tumor regions were irradiated with a 808nm laser at a power density of 2 W/cm^2 of the three NIR groups. The irradiation process contained four consecutive 10 s applications with a 3 minute interval. Tumor size was measured everyday using a vernier calliper for 14 days after the treatment. The tumor volume was calculated according to the following equation: $\text{length} \times \text{width}^2 / 2$. And the tumors were taken photos at days 0,5,10 and 14. Body weights were monitored every three days.

Histological Examination

The tumor of each mouse were harvested after treatment and cut into $8 \mu\text{m}$ slices. Hematoxylin and Eosin (HE) staining and Terminal Deoxynucleotidyl Transferase dUTP nick end labeling (TUNEL) assays were used to stain the tumor slices and examined by the confocal fluorescence microscope (OLYMPUS FV1000). The TUNEL staining was following the manual instruction of TUNEL kit (Roche, Switzerland).

Statistical methods

Data was analyzed by one-way analysis of variance for multiple groups, two-sided Student's t-test for two groups, Statistical significance value was set at $p < 0.05$.

Results and Discussion

Synthesis and characterization of PFTBA@PEG-IR780-C13

Taking into consideration that IR780 with poor solubility (28), we modified the NIR dyes with PEG and long carbon chain. The modified materials PEG-IR780-C13 were prepared following our previous work. Then we used the obtained material PEG-IR780-C13 to encapsulate perfluorotributylamine (PFTBA), which has been used as artificial blood substitute. We prepared the nanosystem PFTBA@PEG-IR780-C13 by emulsification. The hydrophilic shell encapsulated PFTBA in the core position. Transmission electron microscopic (TEM) images showed the uniform particles of 100-600nm in diameter (Figure 1A). Via dynamic light scattering

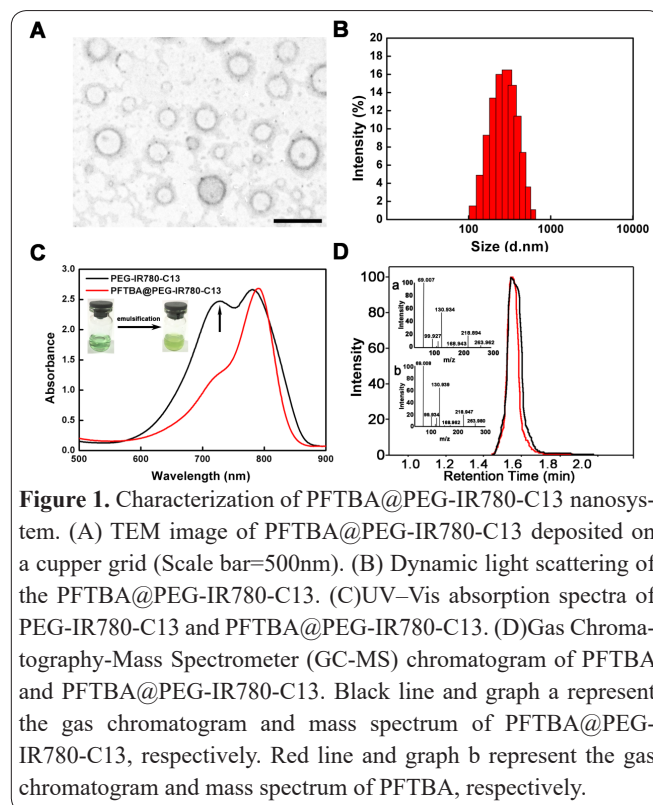


Figure 1. Characterization of PFTBA@PEG-IR780-C13 nanosystem. (A) TEM image of PFTBA@PEG-IR780-C13 deposited on a copper grid (Scale bar=500nm). (B) Dynamic light scattering of the PFTBA@PEG-IR780-C13. (C) UV-Vis absorption spectra of PEG-IR780-C13 and PFTBA@PEG-IR780-C13. (D) Gas Chromatography-Mass Spectrometer (GC-MS) chromatogram of PFTBA and PFTBA@PEG-IR780-C13. Black line and graph a represent the gas chromatogram and mass spectrum of PFTBA@PEG-IR780-C13, respectively. Red line and graph b represent the gas chromatogram and mass spectrum of PFTBA, respectively.

(DLS) measurement, it was found the average size of nanodroplets significant enlarged from 113 nm (data not shown) for the material self-assembled micelles, to 255 nm for the PFTBA@PEG-IR780-C13 (Figure 1B), resulting from the encapsulation of PFTBA. Next, we used the Gas Chromatography-Mass Spectrometer (GC-MS) chromatogram and got results which also revealed the successful encapsulation of PFTBA into PEG-IR780-C13 (Figure 1D).

The formed PFTBA@PEG-IR780-C13 showed similar optical property with PEG-IR780-C13, UV-Vis-NIR absorbance spectra (Figure 1C) revealed the strong absorbance peak (at $\approx 780 \text{ nm}$) for PEG-IR780-C13 polymer before and after PFTBA encapsulation, which could be assigned to characteristic peak of IR780. The stability of PFTBA@PEG-IR780-C13 under dark and light condition without significant change compared with PEG-IR780-C13 and perform better than the IR780 dye (Supplement Figure 3, 4). Furthermore, the self-quenching is a major obstacle of photosensitizer in PDT application. After the encapsulation of PFTBA, the self-quenching concentration of photosensitizer increased (Supplement Figure 5), indicating the PFTBA@PEG-IR780-C13 can reduce the self-photoquenching of NIR dye. Besides, previous studies showed that NIR dye was easily to form π - π aggregation in a poor solvent. The π - π interaction of PEG-IR780-C13 aqueous solution resulting the short-wavelength shoulder peak at 730nm (Figure 1C, The arrow points). As shown in Supplement Figure 5, PEG-IR780-C13 displayed stronger absorbance at 730nm than PFTBA@PEG-IR780-C13 at the same concentration, implicating the loading of PFTBA can effectively inhibit the π - π stacking of PEG-IR780-C13 in aqueous solution.

We further evaluated the fluorescence spectra of PEG-IR780-C13 and PFTBA@PEG-IR780-C13. As shown in Figure 2A, the fluorescence emission of PEG-IR780-C13 quenched obviously, due to π - π stacking of

PEG-IR780-C13 in aqueous solution. After encapsulation of PFTBA, the fluorescence intensity of PEG-IR780-C13 significantly increased. Meanwhile, the fluorescence intensity increased along with the adding amount of PFTBA. Same results can be obtained by using the IVIS Lumina imaging system. Further illustrated encapsulating PFTBA can reduce the π - π stacking of PEG-IR780-C13. This similarity indicates that aggregation does not occur in nanoparticles.

The enhanced $^1\text{O}_2$ production determination in vitro

The single oxygen ($^1\text{O}_2$), one species of reactive oxygen, effectively damages the structure and function of cancer cells. The $^1\text{O}_2$ production ability of PS is a key role in determining the effectiveness in PDT. Thus, we determined the $^1\text{O}_2$ production abilities of PEG-IR780-C13 and PFTBA@PEG-IR780-C13 in vitro by a commercial $^1\text{O}_2$ specific dye, singlet oxygen sensor green (SOSG). It can react with $^1\text{O}_2$ and produce strong fluorescence endoperoxides, which can be determined by photomultiplier tube. We measured the fluorescence signal extent of PEG-IR780-C13 and PFTBA@PEG-IR780-C13 (the concentration of PEG-IR780-C13=50ug/ml, PFTBA=1%, v/v %) by an 808nm laser irradiation for 10s intervals (Figure 2A) after mixing with SOSG. The results shown the fluorescence signal of PFTBA@PEG-IR780-C13 is much higher than PEG-IR780-C13 (Figure 2B). Then we measured a range of different amount of PEG-IR780-C13 and PFTBA (Figure 2C). The dilution caused a remarkable fluorescence decay of PEG-IR780-C13 and PFTBA@PEG-IR780-C13 after 20s irradiation. The largely enhanced $^1\text{O}_2$ generation

ability of PFTBA@PEG-IR780-C13 guaranteed us to use the nanosystem for photodynamic cancer treatment.

To confirm the presence of PFTBA is a key role in enhancing the $^1\text{O}_2$ generation, we firstly measured the fluorescence signal extent of PFTBA@PEG-IR780-C13 by varying the adding amount of PFTBA (0.5% v/v and 1% v/v, respectively). Then we investigated the fluorescence signal intensity by adding two times of PFTBA (0.5% v/v +0.5% v/v) to reach the amount to 1% v/v. The results shown the fluorescence signal extent of two adding ways was similar. And with the increasing of PFTBA adding amount (from 0.5% to 1%), the fluorescence intensity was significantly increased (Figure 2D), which indicating the enhanced $^1\text{O}_2$ production contributed by PFTBA. Besides, as shown in Supplement Table 1, the singlet oxygen quantum yields (Φ_{so}) reflects the $^1\text{O}_2$ production ability of photosensitizer we noticed that after encapsulation the Φ_{so} of PFTBA@PEG-IR780-C13 is much higher compared with PEG-IR780-C13 alone, which demonstrated the encapsulation of PFTBA can improve the $^1\text{O}_2$ production of photosensitizer. Maybe due to the dissolving O_2 ability of PFTBA is much higher than water. (Supplement Figure 2)

In vitro cell experiments

Carboxy- H_2DCFDA , a widely used fluorogenic marker for reactive oxygen species (ROS), was used to evaluate the production of ROS in live cells. We used this fluorescent probe to determinate the ROS generation ability in cellular level. We treated cells with PBS, PEG-IR780-C13 and PFTBA@PEG-IR780-C13, with or without 808nm Laser irradiation. In Figure 3A, Cells treated with PBS, PEG-IR780-C13 and PFTBA@PEG-IR780-C13 showed a negligible fluorescence without Laser irradiation. After laser irradiation, cells treated with PFTBA@PEG-IR780-C13 showed significant green fluorescence while cells treated with PBS and PEG-IR780-C13 still showed negligible fluorescence. The quantitative image analysis showed the fluorescence intensity of PFTBA@PEG-IR780-C13 was much higher than other groups (Supplement Figure 6). To further verify the results, we quantified the percentage of cells stained with Carboxy- H_2DCFDA by flow cytometry (Figure 3B). Cells incubated with PBS, PEG-IR780-C13 showed a relatively low percentage (0.180%, 0.234% and 3.95%, respectively) of green fluorescent signal before irradiation. After irradiation, cells treated with PEG-IR780-C13 showed a slightly increased percentage (24.8%). While the percentage cells treated with PFTBA@PEG-IR780-C13 obviously increased and reached to 82.6%, indicating the better performance of PFTBA@PEG-IR780-C13 as the $^1\text{O}_2$ producer in cells and further potential application for PDT therapy.

The fluorescence imaging of cells co-stained with Calcein AM and propidium iodide confirmed the high PDT efficacy of PFTBA@PEG-IR780-C13 in cancer cell ablation. Live cells stained by Calcein AM shown in green fluorescence while the Dead cells stained by propidium iodide exhibited red fluorescence. As shown in Figure 3C, the red fluorescence can be obviously observed in the group treated with PFTBA@PEG-IR780-C13 and laser irradiation, indicating the great performance of PFTBA@PEG-IR780-C13 (after laser

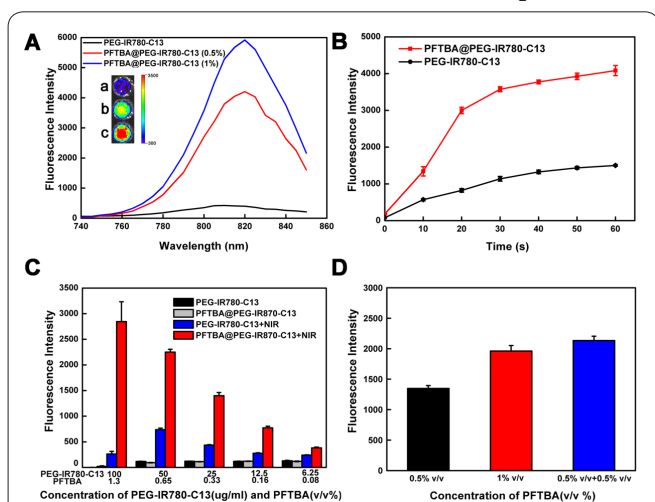


Figure 2. The fluorescence spectra and determination of $^1\text{O}_2$ production. (A) The fluorescence spectra of PEG-IR780-C13, PFTBA@PEG-IR780-C13. The equivalent PEG-IR780-C13 concentration at 50ug/ml, PFTBA amount is 0, 0.5% and 1% (v/v %), respectively. The inset picture was the same samples measured by IVIS Lumina imaging system. (B) $^1\text{O}_2$ production of PEG-IR780-C13 and PFTBA@PEG-IR780-C13 under laser irradiation (808nm, 2w/cm²) as determined by the fluorescence intensity of SOSG. (PEG-IR780-C13=50ug/ml, PFTBA=1%, v/v, n=3). (C) $^1\text{O}_2$ production in different concentration samples. The concentration of PEG-IR780-C13 varied from 100ug/ml to 6.25ug/ml and PFTBA from 1.3% to 0.08% (v/v%), respectively (n=3). The irradiation time is 20s. (D) $^1\text{O}_2$ production in different amount of PFTBA samples. The equivalent concentration of PEG-IR780-C13 is 50ug/ml. The amount of PFTBA varied from 0.5%, 1% and 1% (0.5%+0.5%), respectively. The irradiation time is 10s.

irradiation) in cancer-killing. On the contrary, strong green fluorescence signal obtained in other five groups, demonstrating the relatively useless to cause cancer cell death. These experiments indicated the significant enhanced phototoxicity of PBCs.

The effect of PDT was then studied *in vitro*. Renca cells was treated with PBS and different concentrations of PEG-IR780-C13 or PFTBA@PEG-IR780-C13. Without laser irradiation, no significant toxicity was found in both two groups at different concentrations (Figure 3D). Then we explored the phototoxicity of PEG-IR780-C13 and PFTBA@PEG-IR780-C13. Cell viability with 40s discontinuous 808nm light treatment after incubate with different concentrations of the above two agents were measured. After laser irradiation, we detected a reduction in the viability of cells treated with PFTBA@PEG-IR780-C13 (Figure 3E). And it is notable that the reduction in viability were higher in cells treated with PFTBA@PEG-IR780-C13 than in cells treated with PEG-IR780-C13, demonstrating a robust increase in cell death treated with PFTBA@PEG-IR780-C13 and laser irradiation. Meanwhile, we assessed the photothermal effects of PEG-IR780-C13 and PFTBA@PEG-IR780-C13 *in vitro* (Supplement Figure 7). They showed similar temperature increase (from 22°C to 38°C) after irradiation, indicating the encapsulation process did not change the photothermal property of PEG-IR780-C13. Generally, the treatment temperature in photothermal therapy should rise over 40°C and lasting few minutes (29-31). In our experimental condition, the temperature can only reached about 35°C. It demonstrated the therapeutical agent damaged cancer cells without significantly hyperthermia. In addition, we verified the fragmented, decomposed products of PFTBA@PEG-IR780-C13 after NIR irradiation were not cytotoxic (Supplement Figure 8). After NIR irradiation, it could kill cancer cells through the intracellular generation of 1O_2 . Intracellular trafficking of PFTBA@PEG-IR780-C13 was also studied by using confocal scanning laser microscope. PFTBA@PEG-IR780-C13 was largely enriched in lysosome (Supplement Figure 9). These *in vitro* cell studies demonstrated that PFTBA@PEG-IR780-C13 could be uptake by cancer cells.

In vivo PDT

We further evaluated the PDT effect of PFTBA@PEG-IR780-C13 *in vivo*. The CT26 tumor-bearing mice were divided in six groups, including saline, PEG-IR780-C13 and PFTBA@PEG-IR780-C13 groups with or without laser irradiation. To avoid the potential photothermal effects, we tested the photothermal effect of PFTBA@PEG-IR780-C13 *in vivo* (Supplement Figure 10) and divided the irradiation time into four consecutive 10 s applications with a 3 minute interval. Tumor volumes and body weights were monitored every day. As expected, the tumor growth rate of mice receiving PFTBA@PEG-IR780-C13 and laser irradiation was remarkably reduced after the treatment process (Figure 4A). While the other five groups showed similar tumor growth rate without significant reduction. It demonstrated the PDT effectiveness of PFTBA@PEG-IR780-C13 plus NIR irradiation. Laser or PEG-IR-780, PFTBA@PEG-IR780-C13 did not affect the development of tumor. And the tumor size of PFTBA@PEG-IR780-

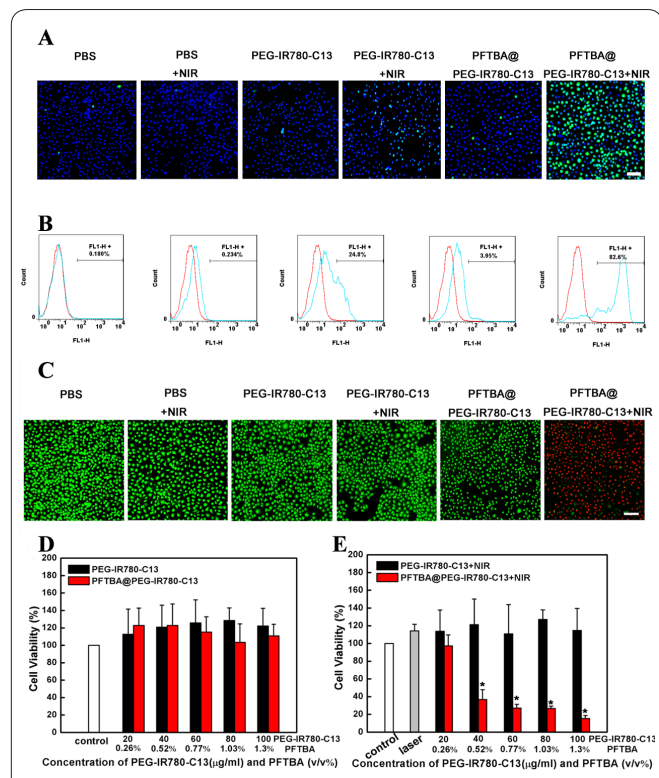


Figure 3. *In vitro* PDT therapy. (A) Cells were treated with different agents and then exposed to an 808nm NIR laser (2 W/cm^2) for 40 s. ROS generation was detected using carboxy- H_2DCFDA . Fluorescence images showing green fluorescence indicate positive staining for ROS; the nuclear of the cells are shown by blue fluorescence indicative of counterstaining with Hoechst 33342 (scale bar=50µm). (B) Flow-cytometry analysis of ROS generation in cells treated with PEG-IR780-C13 and PFTBA@PEG-IR780-C13 and then exposed to 808-nm NIR laser (2 W/cm^2 for 40s) detected using carboxy- H_2DCFDA . (C) Fluorescence microscope images of Calcein AM and PI co-stained Renca cells after various treatments indicated. Green and red colors represented live and dead cells, respectively (scale bar= 50µm). (D) Without or (E) with 808nm light exposure at the power density of 2 W/cm^2 for 40s.

C13+NIR group was relatively smaller than other groups after 14 days treatment progress. Besides, the body weight variation was not significantly observed after the treatment (Figure 4B), indicating no acute toxicity of the therapeutical agent.

To further investigate the therapeutic effects of PFTBA@PEG-IR780-C13 down to the cellular level, hematoxylin and eosin (HE) staining (Figure 4C) and TdT-mediated dUTP Nick-End Labeling (TUNEL) (Figure 4D) assays were used to study the microstructure and apoptosis of tumor cells in each experimental group, respectively. Based on the HE and TUNEL staining results, we found a large number of necrosis and apoptosis of tumor cells from the group of PFTBA@PEG-IR780-C13 receiving laser irradiation compared to other groups which was in accordance with the animal tumor volume growth data, indicating the successful destructive effect of tumor cells by PFTBA@PEG-IR780-C13 and NIR irradiation.

For the absorption of NIR laser irradiation, IR780 has a great potential of phototherapy for deep tumor penetration and therapy. A large amount of nanosystems have been used to encapsulate IR780, increasing the solubility in aqueous solution and decreasing the π - π interaction themselves, which result in increased

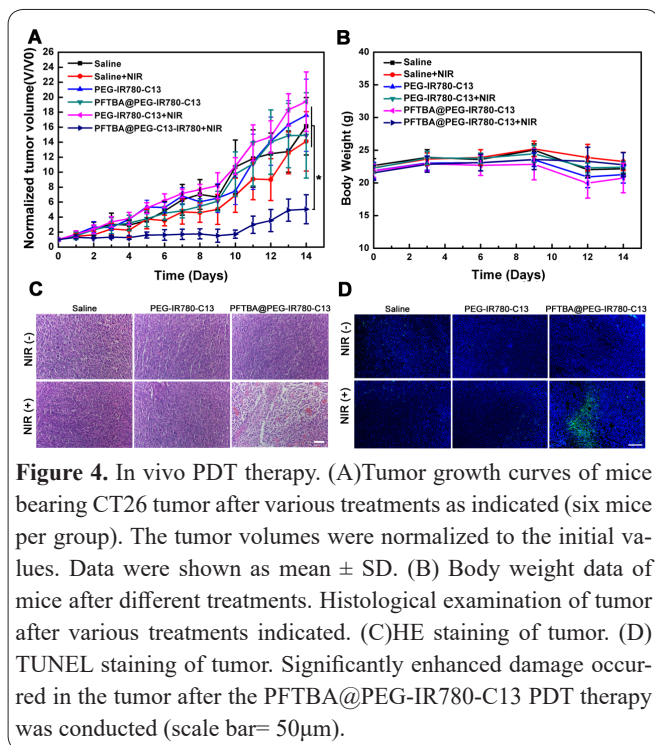


Figure 4. In vivo PDT therapy. (A) Tumor growth curves of mice bearing CT26 tumor after various treatments as indicated (six mice per group). The tumor volumes were normalized to the initial values. Data were shown as mean \pm SD. (B) Body weight data of mice after different treatments. Histological examination of tumor after various treatments indicated. (C) HE staining of tumor. (D) TUNEL staining of tumor. Significantly enhanced damage occurred in the tumor after the PFTBA@PEG-IR780-C13 PDT therapy was conducted (scale bar = 50 μ m).

$^1\text{O}_2$ quantum yield (Φ_{so}). In order to achieve even high $^1\text{O}_2$ quantum yield (Φ_{so}) and more PDT effect of the IR780, perfluorocarbon (PFC) have been used in combination with the IR780. The PFC was approved by FDA as artificial blood, it can delivery oxygen for clinical application. Our previous studies have confirmed oxygen self-enriched PFC can enhance $^1\text{O}_2$ of IR780 due to its high oxygen capacity. Meanwhile, PEGylated IR780 can increase the water solubility of IR780 effectively and decrease the immunogenicity. In this study, we used PFC to generate more $^1\text{O}_2$ of PEGylated IR780 in vitro (Figure 3) by means of combining the PFC and the PEGylated IR780. The nanosystem (PFTBA@PEG-IR780-C13) decreased the π - π interaction peak with little change of the 780nm absorbance (Figure 1C). More importantly, PFC can protect $^1\text{O}_2$ by extending its lifetime about 200 times. Therefore, the oxygen carrier PFC enhanced the $^1\text{O}_2$ generation and the PDT effect by the way of constructing the PFTBA@PEG-IR780-C13 nanosystem. To a great extent, the developed nanosystem (PFTBA@PEG-IR780-C13) can enhanced the therapeutic PDT effect in vitro and in vivo simultaneously (Figure 3 and Figure 4). And it provided a new platform for developing new therapeutic agents of PDT for anti-tumor treatment.

Interest conflict

There is no conflict of interest to be declared by the author.

Author's contribution

All work was done by the author named in this article and the authors accept all liability resulting from claims which related to this article and its contents. The study was conceived and designed by Yiqiao Hu, Jinhui Wu; Huanhuan Zhang, Ahu Yuan collected and analysed the data; Ke Jiang, Haoran Wang wrote the text and all authors have read and approved the text prior to publication.

References

- Zhou Z, Song J, Nie L, Chen X. Reactive oxygen species generating systems meeting challenges of photodynamic cancer therapy. *Chem Soc Rev* 2016; 45(23): 6597-6626.
- Rai P, Mallidi S, Zheng X, Rahmanzadeh R, Mir Y, Elrington S, et al. Development and applications of photo-triggered theranostic agents. *Adv Drug Deliv Rev* 2010; 62: 1094-1124.
- Cheng L, Wang C, Feng L, Yang K, Liu Z. Functional nanomaterials for phototherapies of cancer. *Chem Rev* 2014; 114: 10869-10939.
- Dolmans DEJGJ, Fukumura D, Jain RK. Photodynamic therapy for cancer. *Nat Rev Cancer* 2003; 3: 380.
- Lucky SS, Soo KC, Zhang Y. Nanoparticles in Photodynamic Therapy. *Chem Rev* 2015; 115: 1990-2042.
- Jiang C, Cheng H, Yuan A, Tang X, Wu J, Hu Y. Hydrophobic IR780 encapsulated in biodegradable human serum albumin nanoparticles for photothermal and photodynamic therapy. *Acta Biomater* 2015; 14: 61-69.
- Wang K, Zhang Y, Wang J, Yuan A, Sun M, Wu J, et al. Self-assembled IR780-loaded transferrin nanoparticles as an imaging, targeting and PDT/PTT agent for cancer therapy. *Sci Rep* 2016; 6: 27421.
- Cheng Y, Doane TL, Chuang CH, Ziady A, Burda C. Near Infrared Light-Triggered Drug Generation and Release from Gold Nanoparticle Carriers for Photodynamic Therapy. *Small* 2014; 10: 1799-1804.
- Cui S, Yin D, Chen Y, Di Y, Chen H, Ma Y, et al. In Vivo Targeted Deep-Tissue Photodynamic Therapy Based on Near-Infrared Light Triggered Upconversion Nanoconstruct. *ACS Nano* 2013; 7: 676-688.
- Chen G, Jaskula-Sztul R, Esquibel CR, Lou I, Zheng Q, Dammalapati A, et al. Neuroendocrine Tumor-Targeted Upconversion Nanoparticle-Based Micelles for Simultaneous NIR-Controlled Combination Chemotherapy and Photodynamic Therapy, and Fluorescence Imaging. *Adv Funct Mater* 2017; 27: 1604671.
- Fan W, Yung B, Huang P, Chen X. Nanotechnology for Multimodal Synergistic Cancer Therapy. *Chem Rev* 2017; 117: 13566-13638.
- Huang Y, Qiu F, Shen L, Chen D, Su Y, Yang C, et al. Combining Two-Photon-Activated Fluorescence Resonance Energy Transfer and Near-Infrared Photothermal Effect of Unimolecular Micelles for Enhanced Photodynamic Therapy. *ACS nano* 2016; 10: 10489-10499.
- Rurack, K and M, Spieles. Fluorescence Quantum Yields of a Series of Red and Near-Infrared Dyes Emitting at 600–1000 nm. *Anal Chem* 2011; 83(4): 1232-1242.
- Ren H, Liu J, Li Y, Wang H, Ge S, Yuan A, et al. Oxygen self-enriched nanoparticles functionalized with erythrocyte membranes for long circulation and enhanced phototherapy. *Acta Biomater* 2017; 59: 269-282.
- Ren H, Liu J, Su F, Ge S, Yuan A, Dai W, et al. Relighting Photosensitizers by Synergistic Integration of Albumin and Perfluorocarbon for Enhanced Photodynamic Therapy. *ACS Appl Mater Interf* 2017; 9: 3463-3473.
- Lovell JF, Jin CS, Huynh E, Jin H, Kim C, Rubinstein JL, et al. Porphysome nanovesicles generated by porphyrin bilayers for use as multimodal biophotonic contrast agents. *Nat Mater* 2011; 10: 324.
- Lovell JF, Jin CS, Huynh E, MacDonald TD, Cao W, Zheng G. Enzymatic Regioselection for the Synthesis and Biodegradation of Porphysome Nanovesicles. *Angew Chem Int Ed* 2012; 51: 2429-2433.
- Liang X, Li X, Yue X, Dai Z. Conjugation of Porphyrin to Nano-hybrid Cerasomes for Photodynamic Diagnosis and Therapy of Can-

- cer. *Angew Chem Int Ed* 2011; 50: 11622-11627.
19. Yuan A, Qiu X, Tang X, Liu W, Wu J, Hu Y. Self-assembled PEG-IR-780-C13 micelle as a targeting, safe and highly-effective photothermal agent for in vivo imaging and cancer therapy. *Biomater* 2015; 51: 184-193.
20. Qiu X, Xu L, Zhang Y, Yuan A, Wang K, Zhao X, et al. Photothermal Ablation of in Situ Renal Tumor by PEG-IR780-C13 Micelles and Near-Infrared Irradiation. *Mol Pharm* 2016; 13: 829-838.
21. Zhang Y, Ang CY, Li M, Tan SY, Qu Q, Zhao Y. Polymeric Pro-drug Grafted Hollow Mesoporous Silica Nanoparticles Encapsulating Near-Infrared Absorbing Dye for Potent Combined Photothermal-Chemotherapy. *ACS Appl Mater Interfaces* 2016; 8: 6869-6879.
22. Zhang Y, Ang CY, Zhao Y. Polymeric nanocarriers incorporating near-infrared absorbing agents for potent photothermal therapy of cancer. *Polym J* 2015; 48: 589.
23. Cheng Y, Cheng H, Jiang C, Qiu X, Wang K, Huan W, et al. Perfluorocarbon nanoparticles enhance reactive oxygen levels and tumour growth inhibition in photodynamic therapy. *Nat Commun* 2015; 6: 8785.
24. Zhang H, Barralet JE. Mimicking oxygen delivery and waste removal functions of blood. *Adv Drug Deliv Rev* 2017; 122: 84-104.
25. Gholipourmalekabadi M, Zhao S, Harrison BS, Mozafari M, Seifalian AM. Oxygen-Generating Biomaterials: A New, Viable Paradigm for Tissue Engineering? *Trends Biotechnol* 2016; 34: 1010-21.
26. Gao M, Liang C, Song X, Chen Q, Jin Q, Wang C, et al. Erythrocyte-Membrane-Enveloped Perfluorocarbon as Nanoscale Artificial Red Blood Cells to Relieve Tumor Hypoxia and Enhance Cancer Radiotherapy. *Adv Mater* 2017; 29: 1701429.
27. Que Y, Liu Y, Tan W, Feng C, Shi P, Li Y, et al. Enhancing Photodynamic Therapy Efficacy by Using Fluorinated Nanoplatfom. *ACS Macro Lett* 2016; 5: 168-173.
28. Chen G, Wang K, Zhou Y, Ding L, Ullah A, Hu Q, et al. Oral Nanostructured Lipid Carriers Loaded with Near-Infrared Dye for Image-Guided Photothermal Therapy. *ACS Appl Mater Interfaces* 2016; 8: 25087-25095.
29. Chen Q, Liang C, Wang X, He J, Li Y, Liu Z. An albumin-based theranostic nano-agent for dual-modal imaging guided photothermal therapy to inhibit lymphatic metastasis of cancer post surgery. *Biomater* 2014; 35: 9355-9362.
30. Cheng L, Yang K, Chen Q, Liu Z. Organic Stealth Nanoparticles for Highly Effective in Vivo Near-Infrared Photothermal Therapy of Cancer. *ACS Nano* 2012; 6: 5605-5613.
31. Yang K, Xu H, Cheng L, Sun C, Wang J, Liu Z. In Vitro and In Vivo Near-Infrared Photothermal Therapy of Cancer Using Polypyrrole Organic Nanoparticles. *Adv Mater* 2012; 24: 5586-5592.